ELSEVIER

Catalysis Today 32 (1996) 337–347

CATALYSIS TODAY

# The mechanism of the synthesis in connection with assignments for a solid reaction cycle of the HPA catalyst during catalytic reactions

T. Ilkenhans [a,*], H. Siegert [a], R. Schlögl [b]

[a] *c/o Röhm GmbH, Kirschenallee, D-64275 Darmstadt, Germany*
[b] *FHI Berlin, Faradayweg 4–6, D-14195 Berlin 11, Germany*

**Abstract**

The mechanisms of the oxide syntheses to $PMo_{12}$ and $PVMo_{11}$ were enlightened by in situ UV/VIS and $^{31}$P-NMR. Different solution stabilities of the products were discovered. After several crystalline phase transformations of the solid at higher temperatures (> 573 K) spectroscopic assignments for defect HPA formation were determined. Water supports reversible restructuring into the intact Keggin structure. As a consequence we propose a model concept for a solid repair cycle of the catalyst.

*Keywords:* Keggin structure; Synthesis; Mechanism; Structure promotor effect; Solid structures and reactivity; Defect structures

## 1. Introduction

Molybdovanadophosphoric acids are used heterogeneous catalysts [1–3] for selective oxidations to organic intermediates as Methacrylic acid on an industrial scale.

Ex situ studies on $PMo_{12}$ of Pettersson [4,5] and other authors show the participation of precursors during the synthesis in dependence of acidity by soluble oxometallate salts. Claims on our presented studies are to clarify in situ the reaction pathways of the formation reaction of the oxide synthesis of the Keggin HPA structure. In this context kinetic and thermodynamic aspects of the different reactions are of interest. We suggest that these findings could help us to find optimization strategies for the catalyst synthesis. Moreover knowledge about the real product distribution with the content of byproducts is required, which was first reported by Maksimovskaya et al. [6].

With detailed knowledge of the solution chemistry there is further motivation to look for parallels to the solid state chemistry for a better understanding of the highly active catalyst $PVMo_{11}$. Only very few spectroscopic studies are known showing assignments of significant structural changes of the Keggin cage after use of different calcination and catalytic reaction conditions.

The structural background of the activation period phenomena and the hot spot problems in the reactor is questionable. The most important

* Corresponding author.


*PII* S0920-5861(96)00218-0

disadvantage for the industrial use is rapid deactivation leading to a short lifetime. In this context this work is additionally a contribution to support the understanding of the active state for practical use.

## 2. Experimental

The synthesis procedure was controlled by an in situ apparatus (Fig. 1) under isothermic conditions. UV/VIS monitoring spectra were recorded by a thermostated through-flow cell (thickness 0.01 mm) with a diode array detector system in a reversal optical unit of a Beckman DU 7400 spectrometer. $^{31}$P-NMR measurements were performed on a thermostated Bruker AMX 400 MHz spectrometer. Dispersed metal oxides were separated by a centrifuge obtaining clear solutions. The samples were immediately analyzed at reaction temperature ($H_3PO_4$ and other initial $P_xMo_y$ precursor are roughly estimated and additionally compared with the corresponding in situ UV/VIS absorptions). XRD data of sealed capillaries were taken with a Stoe Stadi P diffractometer in focusing transmission geometry (CuK$\alpha$ radiation, position-sensitive detector). Solid state MAS-NMR spectra were performed on a Varian VXR 300 at a frequency of 121 MHz (rotation frequency $< 3.5$ kHz, standard 85% $H_3PO_4$). IR spectra were obtained on a Perkin Elmer 283B grating spectrometer with KBr and NaCl pellets (calcined dry samples

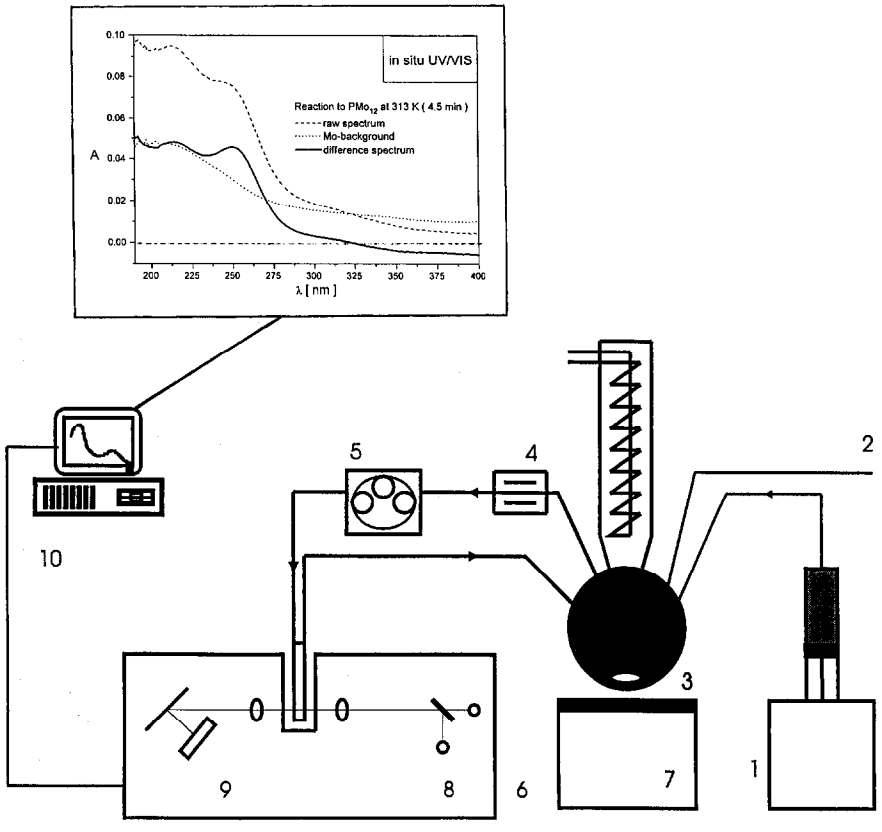


Fig. 1. Scheme of the in situ UV/VIS synthesis apparatus. 1) automatic dose unit, 2) temperature and pH sensors, 3) reaction vessel, 4) through-flow cell for conductometry measurements, 5) tube pump, 6) UV/VIS spectrometer, 7) heating, 8) light sources, 9) diode array detector, 10) computational unit. Inset: in situ UV/VIS spectra at 313 K before and after addition of phosphoric acid. Identification of $P_2Mo_5$ with its $\lambda_{max} = 252$ nm.

were prepared with KBr at 323 K to avoid moisture. Repetition scans were performed after different time delays at room temperature on air). Laser Raman spectra were taken with sealed samples with a Dilor spectrometer (Ar excitation at 488 nm, 5 mW performance).

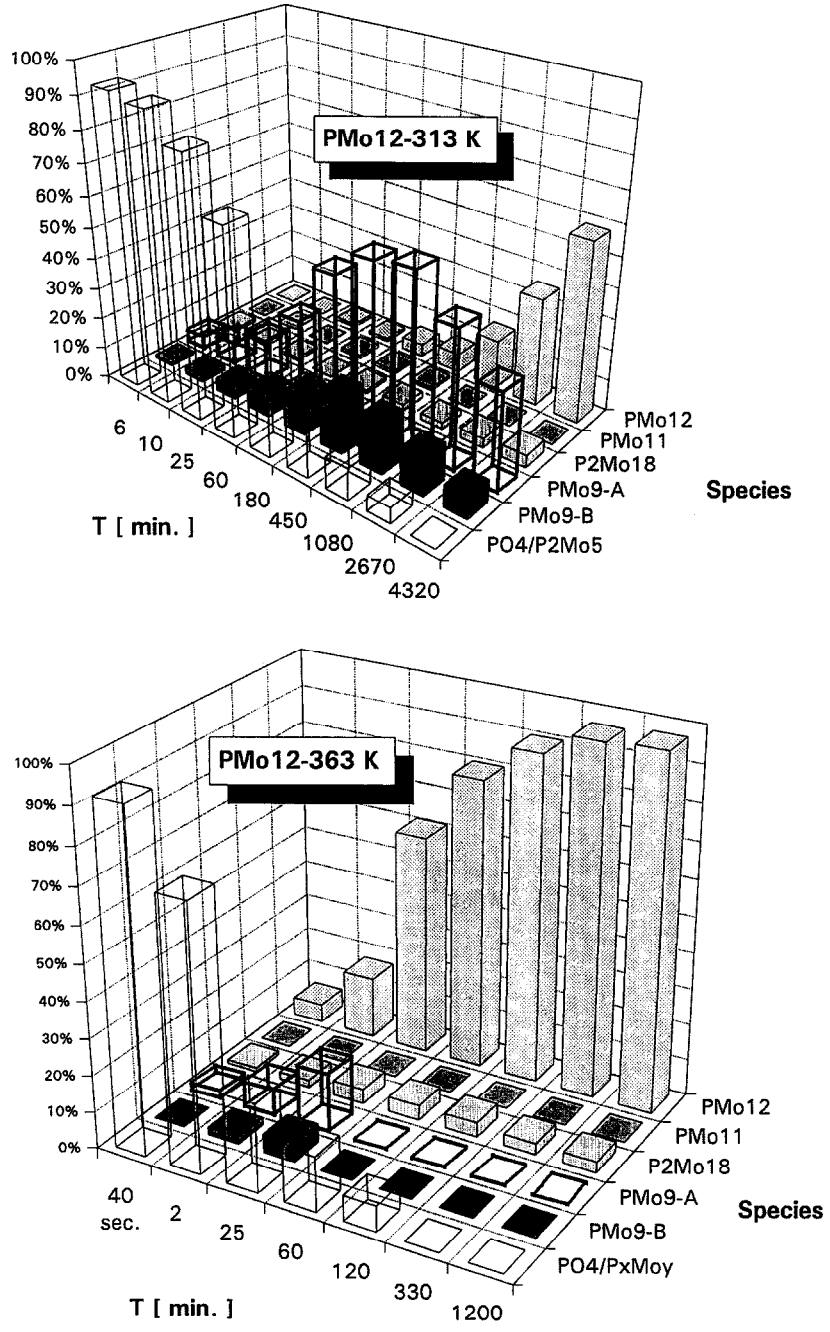


Fig. 2. Top: Quantitative determination of the P containing species distribution by $^{31}$P-NMR spectra in the course of the reaction to $PMo_{12}$ at 313 K. Bottom: The same quantitative determination in the course of the reaction to $PMo_{12}$ at 363 K.

## 3. Results

### 3.1. Synthesis of $PMo_{12}$ and $PVMo_{11}$ with metal oxides

The syntheses (0.0154 molar solution) were conducted with $MoO_3$, $V_2O_5$ and phosphoric acid in water to produce the compounds $H_{3+x}PV_xMo_{12-x}O_{40} \cdot 28\text{–}32H_2O$ ($x = 0\text{–}1$). The mechanism was elucidated by in situ UV/VIS monitoring [7,8] and $^{31}$P-NMR.

At low solution temperature of 313 K the first step is the solution reaction of the oxide to an orthomolybdate $H_{2-x}MoO_4^{x-}$ [8] up to Mo

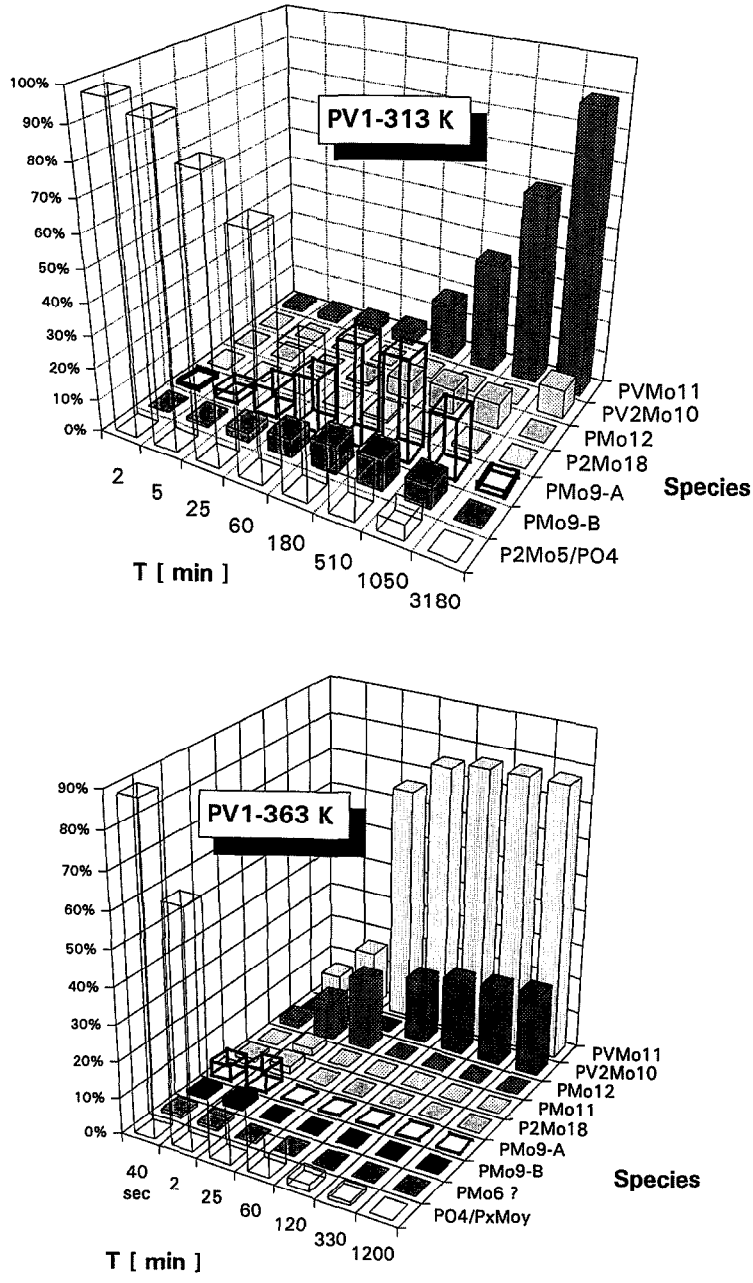


Fig. 3. Top: Quantitative determination of the species distribution by $^{31}$P-NMR data in the course of the reaction to $PVMo_{11}$ at 313 K. Bottom: The same quantitative determination in the course of the reaction to $PVMo_{11}$ at 363 K.

saturation [9] determined by the background in situ UV/VIS spectrum (inset, Fig. 1). At 313 K addition of phosphoric acid leads to the first complexation to the $P_2Mo_5$ precursor ($\lambda_{max}$ 252 nm [10], see inset, Fig. 1). This species is the consequence of the high P/Mo ratio at the beginning of the reaction. The complexation reactions are the incentives for the reaction of the insoluble oxides. In the course of the synthesis of $H_3PMo_{12}O_{40}$ increasing Mo consumption produces the lacunary structure $PMo_9$ [4,11] (see $^{31}$P-NMR spectrum, Fig. 2, top), the most abundant intermediate which is difficult to determine by UV/VIS in the wavelength region above 300 nm only by a shoulder. The precursor $PMo_{11}$ is not stable and disproportionates in the self-acidified solution in $PMo_9$ and $PMo_{12}$. At 313 K even after > 98 h the reaction to $PMo_{12}$ is not complete yielding a broad product distribution. This was also observed by a

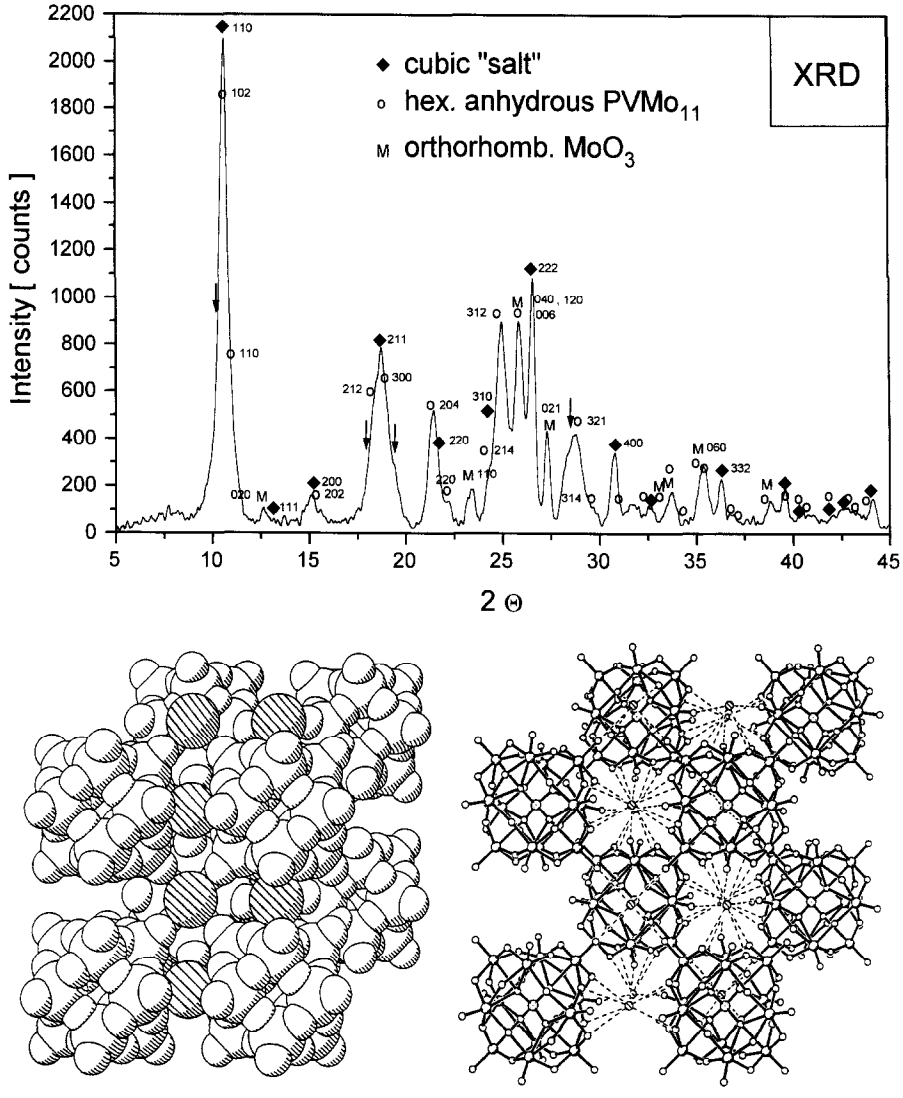


Fig. 4. Top: XRD of $PVMo_{11}$ after calcination on air at 623 K. A mixture of anhydrous structure, cubic salt and orthorhombic $MoO_3$ was observed. The arrows mark unindexed additional reflex angles. Bottom: Simulated structure model for the proposed vanadyl salt structure (cubic, $a$ = 11,6 Å).

strengthened shoulder at 310 nm [8] instead of a clear $\lambda_{max}$ at 310 nm indicating pure $PMo_{12}$ [7].

At 363 K the first step from dissolved orthomolybdate led to an isomolybdate determined by UV/VIS background spectra [7]. At 363 K in Fig. 2 (bottom) it is shown that after addition of phosphoric acid the complexation reactions with direct formation of the intermediate $PMo_9$ and product $PMo_{12}$ begin. At 363 K the reaction is complete. After the reaction and cooling (293 K) the solution of the freshly synthesized $PMo_{12}$ product underlies partial decomposition reactions into a broad product distribution of $PMo_9$, Isomolybdate ($Mo_7$) and $PMo_{12}$. The synthesis and the product composition is never (see also the long-term experiments described in [7]) in a situation of steady state.

The first formation steps of the synthesis to the highly hydrated $H_4PVMo_{11}O_{40}$ proceeds at both temperatures ($^{31}$P-NMR: Fig. 3, top and Fig. 3, bottom) on the same path as for the reaction to $PMo_{12}$. The low solution concentration of V [9] is a reason for the incorporation of $VO_2^+$ into the Keggin structure not before the final step. This was obviously substantiated by the existence of the V-free $PMo_{12}$ as intermediate. Consequently V substitution has no significant effect on the formation rate [8]. In both cases the empirical rate constants at 363 K are $2.7 \times 10^{-5}$ mol $s^{-1}$ $l^{-1}$.

### 3.2. Solid state and catalytic activity

The number of water molecules with their hydrogen bonds between the Keggin cages determine the crystal structures. At 300 K the highest hydrates of the classical Keggin structure $H_3PMo_{12}O_{40} \cdot 28–30\ H_2O$ (space group: $Fd3m$, $a = 23.31$ Å) and tetragonal pseudo-Keggin structure $H_{3+x}PV_xMo_{11-x} \cdot 32–34H_2O$ ($x = 1–5$, RG: $P4/mnc$, $a = 12.89$ Å, $c = 18.44$ Å) were determined [12,13]. The next stage is the triclinic 13-hydrate of $H_4PVMo_{11}O_{40}$ [14] isomorphous to the 13-hydrate of $PMo_{12}$. The cages are connected via hydrogen bonds in a complex network of crystal water. We per-

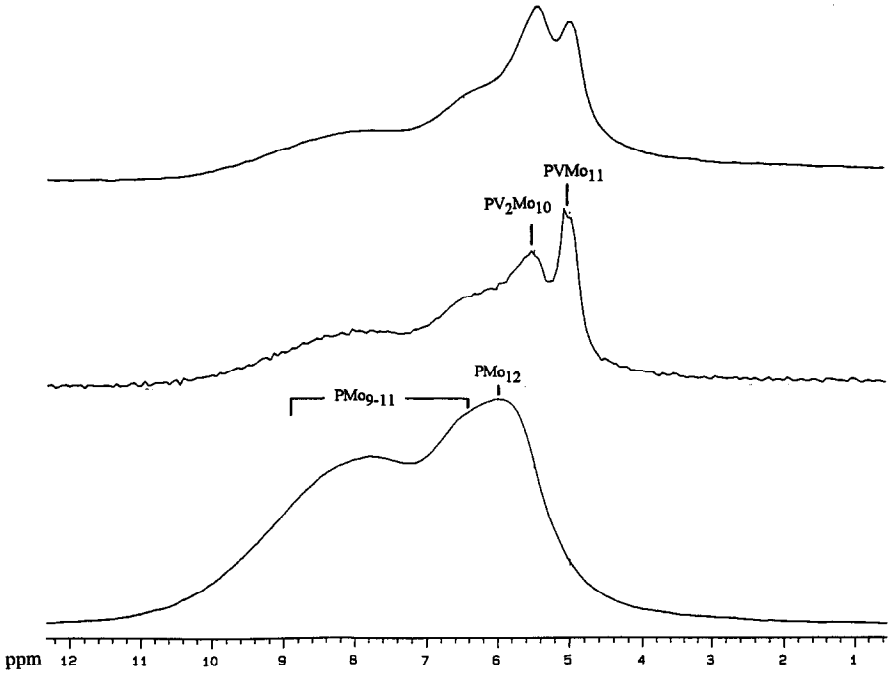


Fig. 5. $^{31}$P-MAS-NMR spectra show after calcination at 568 K a broad product distribution with lacunary structures $PMo_{9-11}$. Rehydration of the same powdered solid sample in moisture leads to restructuring indicated by sharp peaks of the intact Keggin structures.

formed in situ XRD studies [15] under reaction conditions for the oxidative dehydrogenation (ODH) reaction of isobutyric acid to methacrylic acid at 568–593 K showing two other crystalline forms (Fig. 4 top) the anhydrous $H_4PVMo_{11}O_{40} \cdot 0\ H_2O$ (hexagonal [15]) and first of all the cubic structure $H_{4-x}(VO_2^+)_xPV_{1-x}Mo_{11+x}O_{40}$ [15] to be ac-

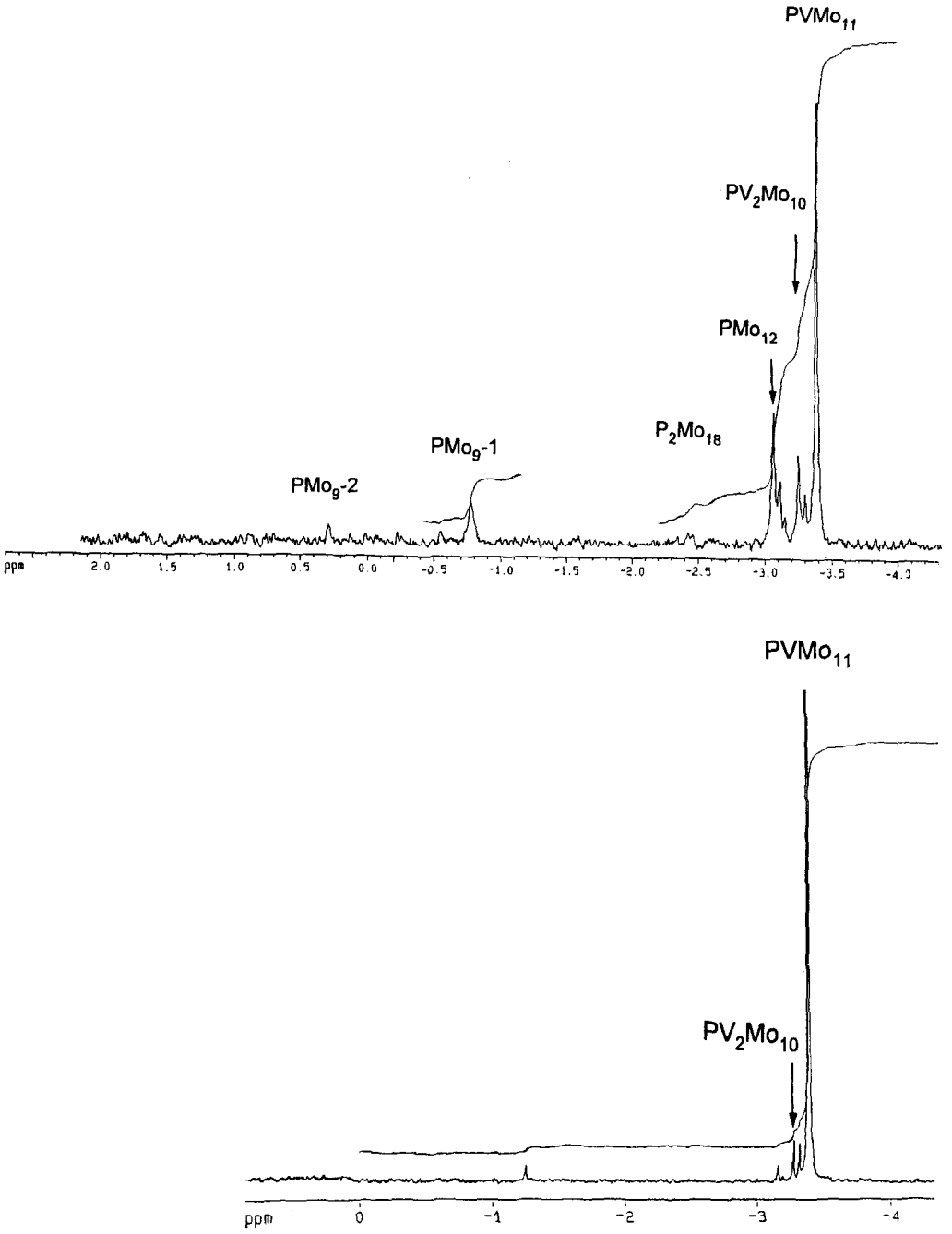


Fig. 6. $^{31}$P-NMR solution spectrum of the cooled (277 K) solution of the calcined samples as in Fig. 5. $PMo_9$ lacunary structures in a significantly broadened product distribution of $PVMo_{11}$ were identified. In the second spectrum at 300 K some minutes later the original product distribution of $PVMo_{11}$ (compare with Fig. 3) appears.

tive. The second structure is isomorphous to the cubic alkaline salt $K_3PMo_{12}O_{40}$ (space group: $Pn3m$, $a = 11.6$ Å [16]). The structure of the $K_3$ salt serve the data for a simulated model of a possible structure in Fig. 4 bottom. Possibly in this structure $VO_2^+$ ions occupy a part of the cationic sites at the polyanions. By then both structures contain no water of crystallisation. V disintegration out of the primary structure was also substantiated by EDX in case of still active catalysts in a highly reduced state [7].

After calcination at 568 K $^{31}$P-MAS-NMR spectra (Fig. 5) show a broad product distribution. Rehydration of the same powdered solid sample in moisture leads to restructuring of a majority of assumed defects into intact $PV_x$ Keggin structures. In cooled solutions of the same calcined samples (277 K, $^{31}$P-NMR solution spectrum, see Fig. 6, top) the knowledge of literature spectra [5] led us to the conclusion that $PMo_9$ lacunary structures appear in a significantly broadened distribution of different species. At 300 K thirty minutes later after complete restructuring the original product solution distribution of $PVMo_{11}$ appears in the second spectrum.

In the Raman spectra (Fig. 7 [17]) we observed strongly changed spectra of $PVMo_{11}$ in the same way for samples calcined at 573–623 K as described before. The assumption that these structures are lacunary structures is supported by a comparison of spectra of known lacunary structures. Characteristic peak positions for $PMo_9$ ($Mo = O_t$) are 975–984 $cm^{-1}$ [18] and at 1038 $cm^{-1}$ for $PMo_{11}$ (compare with IR in Fig. 8). For a distinction from the intact Keggin structures the $Mo = O_t$ peak at 1005 $cm^{-1}$ etc. is used (see also $MoO_3$ = M [19]).

In Fig. 8 in the course of calcination above 593 K the IR spectra (transmission) of the intact HPA with their known vibrations [20] are also strongly affected. A new peak at 1035 $cm^{-1}$ and broadened peaks of $\nu_{as}$P–O at 1070 $cm^{-1}$ and $Mo = O_t$ 960–1000 $cm^{-1}$ become visible. Literature spectra of comparable defects as $La(PMo_{11})_2$ [21] and a $ZnPMo_{11}$ derivative [22] reveal the same splitting which were deduced to the $\nu_{as}$P–O vibrations. In air at 300 K 15–20

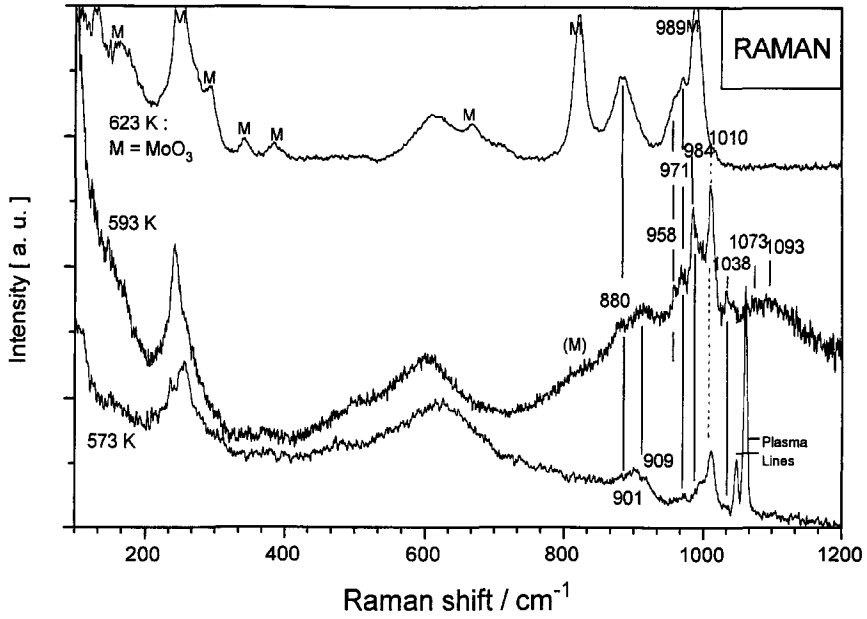


Fig. 7. Raman spectra of $PVMo_{11}$: Above 593 K significant changes visible up to 623–673 K. Literature spectra [19] of prepared $PMo_{9-11}$-lacunary compounds are in good agreement with peaks at 958–984 and 1038 $cm^{-1}$. Above this temperature region $MoO_3$ (M) predominates.

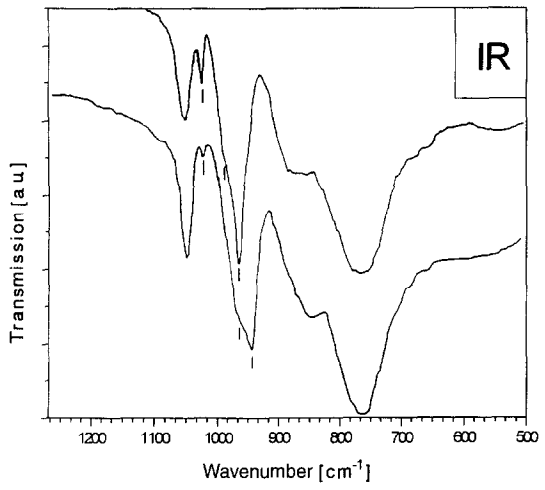


Fig. 8. IR spectra of $PVMo_{11}$ samples calcined at 593 K (KBr pellet, the 323 K warm sample was immediately measured). Additional intense peak at 1035 cm$^{-1}$ and region at 960–70 cm$^{-1}$ give clear assignments [21,22] for a $PMo_{11}$ defect structure. At 300 K the additional peaks decrease significantly under strengthening of the intact Keggin structure vibrations (e.g. at 1070 cm$^{-1}$).

min later, the additional peak of the same KBr pellet weakens and vanishes.

As shown by the in situ study the observed structural changes with the formation of $MoO_3$ at the end of deactivation occur in the temperature region of high catalytic activity for the ODH reaction, acrolein and methacrolein oxidation and in particular for the oxidation of paraffins like isobutane. For example at 573–593 K the conversion of isobutyric acid on $Cu_{0-0.06}PVMo_{11}$ is 70%, maximal selectivity of 69% ($W/F = 2$ h, feed: 5% IBA, 10% $O_2$, 10% $H_2O$, 75% $N_2$). Especially in the hot spot zone of the integral tube reactor the temperature can be up to 40–70 K higher than that adjusted outside the tube in the salt bath. Water stabilized the high activity in a very significant way for a long time period. Ex situ samples of the used still active catalyst exhibit crystals of the cubic HPA 'salt' structure, weakly crystalline, amorphous material (XRD: broad unknown reflex angles) and crystalline $MoO_3$ indicating very similar solid reactivity as observed during calcination experiments [23].

## 4. Discussion

For the reacted $PV_xMo_{12-x}$ product solution we find a significant structure promotor effect. This is an important difference between $PMo_{12}$ and $PV_xMo_{12-x}$. For the moderate sharp product distribution of $PVMo_{11}$ we observed a reversible temperature behaviour (steady state) between the quantities of the intact Keggin structures $PVMo_{11}$ and $PV_2Mo_{10}/PMo_{12}$ on the other hand (compare both spectra in Fig. 3). The quantitative compositions change significantly in reproducible limits. Additionally in other experiments a concentration dependency was observed [7,8].

In connection with the different crystal structures in our opinion the stronger hydration of $PVMo_{11}O_{40}^{4-}$ in comparison with $PMo_{12}O_{40}^{3-}$ is a consequence of the one electron higher elementary charge/cage radius ratio of the $H_4PVMo_{11}$ cage. Therefore the higher hydration energy is a plausible reason for the higher stability of the $PV_x$ species in solution. We describe this fact as structure promotor effect of V. A higher stability for new synthesized highly condensed $Mo_{154}$ polyoxometallate compounds in comparison with monomeric precursors was found by Müller et al. [24]. In this case the explanation for the condensations was also concluded from a higher hydration energy.

Solid structure studies reveal spectroscopic information about stepwise processes during thermal decomposition. $^{31}$P-MAS-NMR and $^{31}$P-NMR solution spectra show that V disintegration in the presence of water seems to be completely reversible. The presence of $PMo_9$ indicates significant solid reactivity.

Additional peaks, identified by Raman spectroscopy, besides the residual intact HPA peaks were assigned as V disintegration and formation of $PMo_{9-11}$ lacunary structures. An additional interpretation as an $VO^{2+}$ vibration can not be totally excluded, because $V = O_t$ groups absorb at 1030–1040 cm$^{-1}$. On the other hand the loss of an VO group at first causes defects to be left behind.

The reversible IR spectroscopic changes in presence of moisture were interpreted as restructuring and salification of defects with $K^+$ leading to the intact Keggin HPA. Before complete decomposition occurs a temperature region with reversible structural changes exists.

During catalytic tests in the hot spot zone the temperature of the catalyst reaches the temperature region of the total decomposition of the HPA. This fact supports the assumption of the existence of the observed defects under active conditions. Very recently ESR experiments by two groups [25,26] have shown V ejection in the course of the catalysis. Weismantel et al. [26] also found assignments for the reentry after complete reoxidation in the presence of water.

All together the findings are the basis for a model of a solid repair cycle (Scheme 1) for $PV_xMo_{12-x}$. Therefore this initial decomposition products seem to be metastable. The direct participation of these solid reactions on the catalytic reaction is not clear. It could be that the repair cycle is only a consequence of the high grade of reduction during several catalytic reaction cycles by a MVK mechanism model [27]. In a comparable sense reversible crystallographic shearing effects or defects of octahedral metal oxide structure catalysts caused by loss of lattice oxygen occurs. The model concept of a repair cycle involves not only oxygen vacancy refilling by oxygen but it seems to be possible to include the reentry of a metal group as $VO_x$ to form the intact Keggin structure again. Conclusively after calcination we interpret the several spectroscopic changes as defects of the HPA catalyst. This initial decomposition products seem to be metastable.

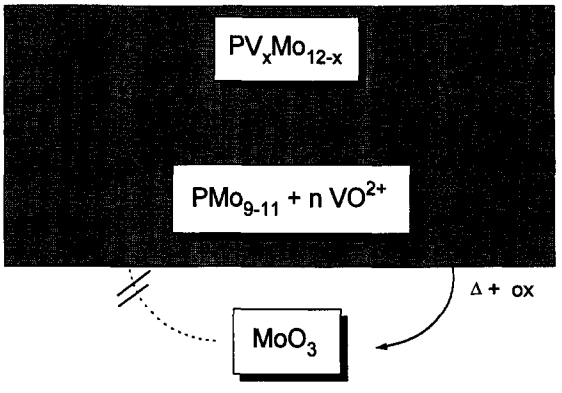


Scheme 1. The model of a repair cycle of the catalyst $PVMo_{11}$. The grey area marks the different Keggin derivative species which exist under the conditions which preserve high catalytic activity. The arrows show the possibility of solid reactions of the species towards each other in a repair cycle.

The formation of highly crystalline $MoO_3$ deactivates [15] the catalyst and seems to be the complete and irreversible 'death' of the HPA catalyst in connection with phase separation. Actually we find no clear assignments for a 'solid synthesis' a generation of crystalline Keggin molybdophosphoric derivatives under reaction conditions [15]. Recently, this solid generation with $MoO_3/SiO_2$ was substantiated by an in situ Raman study for the formation of silicomolybdophosphoric acid $SiMo_{12}$ by Wachs et al. [28] under comparable conditions at $< 573$ K with saturated water pressure.

The complete water loss can be seen as a starting point of the reversal of the formation reaction. In this context the role of water in the feed lies not only in the diluent or in the product desorption function but stabilizes directly the intact (or defect) HPA structure with its hydrogen bonds.

In our opinion the potential for reversible structural change is an important requirement for heterogeneous oxide catalysts for selective oxidation reactions to reach high claims as highest performance and long lifetime.

## 5. Conclusion

The mechanism of the reaction includes $P_2Mo_5$ and the formation of $PMo_9$, the most stable intermediate. In solutions of water we determined a significant structure promotor effect of V for the $PV_x$ Keggin derivatives in comparison with the unstable $PMo_{12}$ compound.

The indications for metastable defect structures in the course of the catalyst decomposition can be considered as a reverse of the synthesis

path. Presence of $H_2O$ under oxidizing conditions induces V reentry in defect holes with restructuring of the intact Keggin structure. These findings cause a model concept for a solid repair cycle of the catalyst.

In summary, the supposed parallels for this catalyst between solution and solid state chemistry seem to be a reality.

## Acknowledgements

This work is a collaboration of the Röhm GmbH (financial support by R. foundation) and Prof. R. Schlögl. The solution NMR were performed with Dr. Zimmermann in the NMR division of the University of Frankfurt/M. Raman experiments were performed in collaboration with D. Spielbauer and G. Mestl at the university of Munich in the group of Prof. H. Knözinger. We acknowledge Dr. E. Bielmeier for ODH catalytic tests and fruitful discussion and Dr. N. Deusch (both Röhm GmbH) for MAS-NMR spectroscopic measurements.

## References

[1] O. Watzenberger, G. Emig and D.T. Lynch, J. Catal., 124 (1990) 247.
[2] G.B. McGarvey and J.B. Moffat, J. Catal., 132 (1991) 100.
[3] D. Casarini, G. Centi, P. Jiru, V. Lena and Z. Tvaruzkova, J. Catal., 143 (1993) 325.
[4] L. Lyhamn and L. Pettersson, Chem. Scr., 16 (1980) 52.
[5] L. Pettersson, I. Andersson and L.-O. Öhman, Inorg. Chem., 25 (1986) 4726.
[6] R.I. Maksimovskaya, M.A. Fedotov, V.M. Mastikhin, L.I. Kuznetsova and K.I. Matveev, Docl. Phys. Chem., 240 (1978) 422.
[7] T. Ilkenhans, Dissertation, Universität Frankfurt/M 1995.
[8] T. Ilkenhans and R. Schlögl, J. Chem. Soc., Faraday Trans., to be published.
[9] Gmelin Handbuch der Anorganischen Chemie, Molybdenum Suppl. Vol. B1, Chapt. 3.5.5.1.6., p. 142, Vanadium Suppl. Vol. B 48, 8th Ed., 1967, p. 97.
[10] T. Hori, J. Inorg. Nucl. Chem., 39 (1977) 2173.
[11] J.A. Rob van Veen, O. Sudmeijer, C.A. Emeis and H. de Wit, J. Chem. Soc., Dalton Trans., (1986) 1825.
[12] V.A. Sergienko, M.A. Porai-Koshits and E.N. Yurchenko, J. Struct. Chem., 21 (1980) 87.
[13] B. Herzog, W. Bensch, T. Ilkenhans, R. Schlögl and N. Deusch, Catal. Lett., 20 (1993) 203.
[14] W. Bensch and T. Ilkenhans, unpublished data;.
[15] T. Ilkenhans, B. Herzog, T. Braun and R. Schlögl, J. Catal., 153 (1995) 275.
[16] J.C.A. Boeyens, G.J. Mc Dougal and J. Van R. Smit, J. Solid State Chem., 18 (1976) 191.
[17] T. Ilkenhans, D. Spielbauer, G. Mestl, H. Knözinger and R. Schlögl, to be published.
[18] L. Lyhamn and L. Pettersson, Chem. Scr., 12 (1977) 142.
[19] H. Knözinger and H. Jeziorowski, J. Phys. Chem., 83 (1979) 9, 1166.
[20] C. Rocchiccioli-Deltcheff and M. Fournier, J. Chem. Soc. Faraday Trans., 87 (1991) 24, 3913.
[21] E.-B. Wang, Y.-K. Shan, Z.-X. Liu and B.-J. Zhang, Acta Chim. Sin., (1991) 774.
[22] R. Massart, R. Contant, J.M. Fruchart, J.P. Ciabrini and M. Fournier, Inorg. Chem., 16 (1977) 2916.
[23] E. Bielmeier and T. Ilkenhans, Röhm GmbH, unpublished data.
[24] A. Müller, E. Krickemeyer, J. Meyer, H. Bögge, F. Peters, W. Plass, E. Diemann, S. Dillinger, F. Nonnenbusch, M. Randerath and C. Menke, Angew. Chem., 107 (1995) 2293.
[25] A. Aboukais, C. Haubtmann, J.J. Andre, C. Desquilles, M. Dourdin, I. Mathes-Juventin-Andrieu, F.C. Aissi and M. Guelton, J. Chem. Soc., Faraday Trans., 91 (1995) 1025.
[26] L. Weismantel, J. Stöckel and G. Emig, Appl. Catal. A, 137 (1996) 129.
[27] P. Mars and D.W. van Krevelen, Chem. Eng. Sci. Suppl., 3 (1954) 41.
[28] M.A. Banares, H. Hu and I.E. Wachs, J. Catal., 155 (1995) 249.